PHYSICAL REVIEW B VOLUME 47, NUMBER 11 15 MARCH 1993-I

# Electron density and structure of the (1×2)-Au(110) surface studied by He-beam scattering

P. Cortona
*Dipartimento di Fisica dell'Università di Genova, Via Dodecaneso 33, 16146 Genova, Italy*

M. G. Dondi
*Istituto di Fisica di Ingegneria dell'Università di Genova, Via Dodecaneso 33, 16146 Genova, Italy*

D. Cvetko* and A. Lausi
*Laboratorio INFM-TASC, Padriciano 99, 34012 Trieste, Italy*

A. Morgante
*Dipartimento di Fisica dell'Università di Trieste and Laboratorio INFM-TASC, Padriciano 99, 34012 Trieste, Italy*

K. C. Prince
*Sincrotrone Trieste S.C.p.A., Padriciano 99, 34012 Trieste, Italy*

F. Tommasini
*Dipartimento di Fisica dell'Università di Trento and Laboratorio INFM-TASC, Padriciano 99, 34012 Trieste, Italy*
(Received 2 June 1992)

The (1×2)-Au(110) surface has been studied using He-beam scattering with time-of-flight detection. The experiments included measurement of the diffraction pattern and the specular intensity as a function of azimuthal angle of incidence; the latter curve is found to be highly structured. The data have been modeled using the local-density approximation to calculate the charge distribution in atoms, and treating the He-surface potential as a superposition of pseudopairwise terms. The diffraction pattern and azimuthal data can be well fitted using close-coupled channel calculations and varying only three parameters, giving confidence that the calculated electron density is accurate. It is found that the peak-to-peak corrugation of the $10^{-3}$ Å$^{-3}$ isoelectron density surface is $\approx$ 1.2 Å, showing a substantial smoothing with respect to the corrugation of 1.55 Å found when superposing the calculated free atomic densities. In addition we have examined the sensitivity of the model calculations to geometric structure. They are consistent only with the expected missing row structure, and yield the separation between the first and second layers with an accuracy of 6%.

## I. INTRODUCTION

He-beam scattering is of wide interest in surface studies due to its particular characteristics. Thermal energy He atoms sample the electron density a few angstroms above the topmost nuclear plane[1,2] thus providing a powerful tool for the characterization of surface reconstructions[3] and defects;[4,5] moreover, He atoms have energy and momentum comparable with those of phonons allowing the vibrations of the topmost layer to be studied with unsurpassed energetic resolution[6,7] by time-of-flight (TOF) measurements. Nevertheless, the analysis of He-surface scattering results still presents a few difficulties due to the role played by the van der Waals forces, in particular in experiments with beam energy close to the potential-well depth. For low corrugation surfaces, the effects of the attractive forces are easily identified in the scattering data as bound-state resonances, giving rise to narrow features in the specular and diffracted intensities centered at a few angles of incidence.[8,9] On the other hand, for highly corrugated surfaces such as oxygen overlayers on Cu(110) (Ref. 10) and Ag(110) (Ref. 11) or the (1×2) phases of the clean Au(110) (Refs. 4 and 12) and Pt(110) (Refs. 3 and 13) surfaces, multiple scattering from the repulsive wall and hopping in the potential well combine to make the scattered intensity highly structured and quite difficult to interpret. In these cases the semiclassical approach to the scattering problem may lead to ambiguous or wrong conclusions and it is necessary to carry out exact calculations of the scattering intensities for realistic choices of the interaction potential. This point was recently considered by Kirsten and Rieder,[13] in a paper dealing with He scattering from the (1×2)-Pt(110) surface. These authors take account phenomenologically of the He-surface interaction potential and compare the scattering data to exact calculations of the scattering probabilities, showing that the corrugation of the attractive part of the potential well plays an important role in the scattering process.

In the present work we consider the (1×2)-Au(110) surface, which was recently the subject of extensive stud-

 

ies by us[4] and others[12,14,15] concerned with the order-disorder deconstruction transition at 700 K. Here we investigate the properties of the $(1 \times 2)$ surface at low temperature. High-resolution He-diffraction patterns taken with the apparatus[7] and the crystal surface previously used in the deconstruction study[4] are reported. Particular attention is given to the behavior of the specular intensity versus the azimuthal angle, which is unusually structured. Experimental details and results are given in Sec. II, while Sec. III deals with the analysis of the experimental data. The analysis is done by using a model of the interaction potential presented recently and shown to be highly accurate in describing the interaction of He with Ag(110) and Cu(110).[16] The model describes the He-surface interaction potential as a superposition of pseudopairwise terms. These are evaluated by starting from calculations of the electron density of the Au free atoms, performed in the local-density approximation with degeneracy-dependent self-interaction correction[17] (D-SIC) and by accounting for the dispersive energy at all orders in the multipolar expansion.[18] The pseudopairwise terms are made anisotropic in order to simulate the rearrangement of the atomic electron cloud which may occur when the metal atom is embedded in the surface environment. As shown in Sec. III, close-coupled channel (CCC) calculations of the scattering probabilities carried out for this model potential are in excellent agreement with the experimental results provided that the anisotropy parameters are properly chosen. We also consider what structural information can be extracted from the data.

A summary is given in Sec. IV. The main result concerns the surface electron density which is accurately determined by the experiment. With respect to the superposition of free-electron densities, a substantial smoothing of the isoelectron density surfaces is observed.

## II. EXPERIMENT

The experimental apparatus, described elsewhere,[7] is provided with a TOF detector positioned in a small vacuum chamber separated from the sample chamber by an aperture. The beam and the detector axis form a fixed angle of 110° and meet at a point where the Au(110) surface is located; the plane containing the beam and the detector axis is hereafter referred to as the scattering plane. The angular resolution of the apparatus is 0.135° full width at half maximum (FWHM), the velocity-spread FWHM reaches 1.2% of the mean velocity for a beam source cooled with liquid nitrogen, and the accuracy in the angular setting and reading is close to 0.01°. The Au single crystal is the one recently used for the study of the order-disorder missing-row deconstruction.[4] After the preparation procedure detailed in Ref. 4, the average distance between monatomic steps separating two well-ordered (1×2) terraces exceeds 200 Å along [001] and is substantially larger along $[1\bar{1}0]$.

Time-of-flight analysis of the atoms reaching the detector is carried out in order to reject the atoms inelastically scattered at the surface. The diffraction pattern taken along the $[1\bar{1}0]$ azimuth, with surface temperature

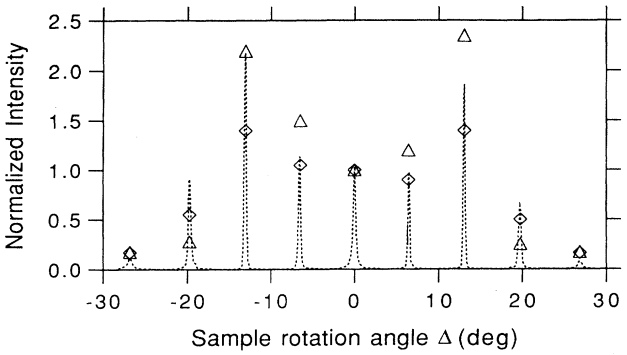


FIG. 1. Diffraction pattern, full line, measured along the [001] azimuth, with surface temperature set at $T_s = -130\,^{\circ}\mathrm{C}$ and with beam wave vector $k = 5.972\ \text{Å}^{-1}$. The angle $\Delta$ is related to the incidence and exit angles as $\Delta = (\Theta_i - \Theta_f)/2$. Calculated peak heights: △, atomic position set according to Ref. 22; ◇, 26% inward relaxation of the topmost layer. The peak heights were calculated from the scattering probabilities by including Debye-Waller attenuation and the measured broadening, and normalizing to the (0,0) peak.

$T_s = -130\,^{\circ}\mathrm{C}$, is reported in Fig. 1 (in this figure the angle $\Delta$ is the rotation angle of the sample and determines the incidence and exit angles which are $\Theta_i = 55° - \Delta$ and $\Theta_f = 55° + \Delta$, respectively).

It appears that the diffraction pattern is typical of the (1×2) reconstruction and that the peak-to-valley intensity ratios exceed $10^4$ in most cases. Similar measurements, taken at several temperatures in the range 140–

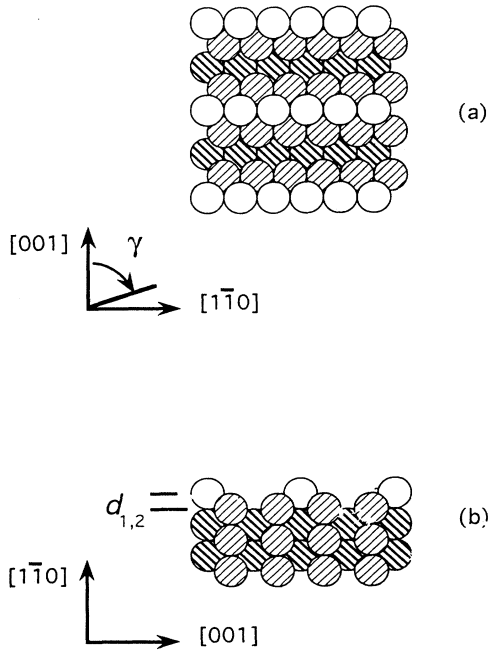


FIG. 2. (a) Top view of the (1×2)-Au(110) surface; in the bottom left corner are shown the in-plane $[1\bar{1}0]$ and [001] axes and azimuthal angle $\gamma$. (b) Side view, showing the first interlayer spacing $d_{12}$; in the bottom left corner are shown the surface normal [110] and the in-plane [001] axis.

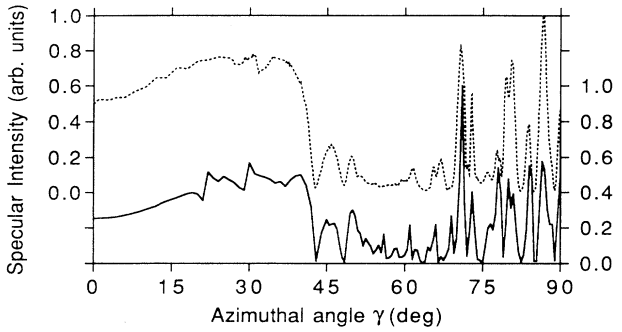


FIG. 3. Comparison of the theoretical and experimental specular intensity as a function of the azimuthal angle $\gamma$. Dotted line, left scale: experiment; full line, right scale: theory.

1100 K were recently reported and analyzed[4] with respect to the behavior of the (1×2) to (1×1) phase transition and to the formation of surface defects. Here attention is focused on the geometry of the atomic structure inside each surface terrace which is responsible for the integrated diffraction intensities (the area below each diffraction peak). The integrated intensities are expected to be independent of the presence of steps and of the velocity spread of the beam.[7]

It is to be noted that all measurements were taken after accurately setting the azimuthal angle $\gamma$, i.e., the angle between the scattering plane and the [001] crystallographic axis, Fig. 2. In fact the specular intensity depends dramatically on $\gamma$ as shown in Fig. 3. In particular around $\gamma = 90$, it changes by two orders of magnitude for a change of the azimuthal angle of 1°.

In the following, the diffraction data reported in Fig. 1 and the behavior of the specular intensity reported in Fig. 3 are shown to provide a quite accurate determination of the He-surface interaction potential and of the surface-electron density, and to provide information about the structure of the surface.

## III. ANALYSIS

### A. Electron density

According to Ref. 16 the He-surface interaction potential can be written as

$$V(\mathbf{R},z)=\sum_{klm}u(\mathbf{r}-\mathbf{r}_{klm}) - \frac{C}{(z-Z_0)^3+\sigma^3\exp[-\frac{1}{2}(\frac{z-Z_0}{\sigma})^3]}, \quad (1)$$

where $\mathbf{r}\equiv(\mathbf{R},z)$ and $\mathbf{r}_{klm}\equiv(\mathbf{R}_{klm},z_k)$ are, respectively, the coordinates of the He atom and of the metal atoms in the $k$th atomic layer. The coordinate $z$ is measured along the surface normal with origin at the topmost nuclear plane. The pseudopairwise potential $u(\mathbf{r}-\mathbf{r}_{klm})$, accounting for the short-range interaction, is written as

$$u(\rho_{klm}) = \eta_x\eta_y A\exp(-\beta\rho_{klm}) \times\{1-\exp[0.36\beta(\rho_{klm}-\sigma)]\}, \quad (2)$$

where $\eta_x$ and $\eta_y$ are anisotropy parameters and

$$\rho_{klm}=\sqrt{(z-z_k)^2+[\eta_x(x-x_{klm})]^2+[\eta_y(y-y_{klm})]^2}. \quad (3)$$

The coordinate $x$ is measured along the rows of close-packed atoms—i.e., parallel to the $\Gamma X$ line in reciprocal space—and the $y$ axis is chosen parallel to $\Gamma Y$ (the $[1\bar{1}0]$ and [001] crystallographic directions, respectively). The second term on the right-hand side of Eq. (1) accounts for the long-range tails of the dispersive energy. As in the previous studies of He-Ag(110) and He-Cu(110) systems[16] the parameters $A$ and $\beta$ are set by starting from D-SIC (Ref. 17) calculations of the electron densities of the free atoms, while $C$ and $Z_0$ are set according to the calculations of Zaremba and Kohn.[19] Therefore $\sigma$, $\eta_x$, and $\eta_y$ are the only parameters to be varied to fit the scattered intensities to the calculated scattering probability.

The D-SIC electron density of Au is shown in Fig. 4. In the range of interest for He scattering, say 2–7 Å, it is approximated with an accuracy of a few percent by $N\exp(-\beta r)$ with $N = 2.88$ Å$^{-3}$ and $\beta = 2.65$ Å$^{-1}$. According to these calculations, and in the framework of the effective-medium approximation,[20,21] we set $\beta$ at the atomic value and $A = \alpha N = 86.4$ eV, while following Zaremba and Kohn we set $C = 275$ meV Å$^3$ and $Z_0 = 0.17$ Å.[19]

The superposition of the pseudopairwise terms in Eq. (1) was first carried out assuming the locations of the gold atoms reported by Moritz and Wolf.[22] Next, for several choices of the parameters $\sigma$, $\eta_x$, and $\eta_y$, the diffraction probabilities and the specular probability as a function of $\gamma$ are evaluated by CCC calculations[23] and compared to the experimental results. The effect of $\eta_x$,

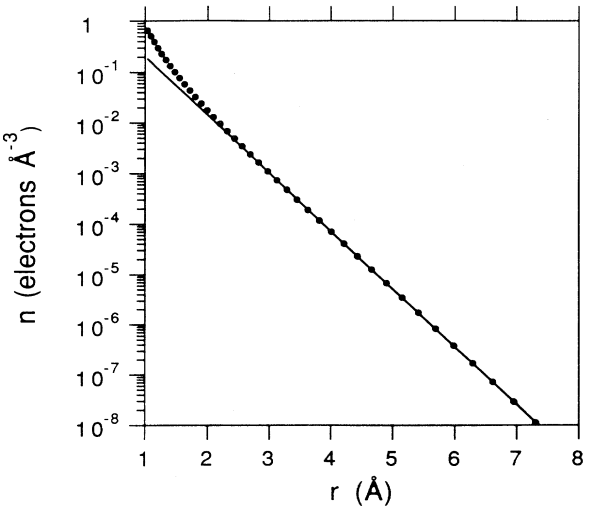


FIG. 4. D-SIC electron density of the Au atom: $r$ is the distance from the nucleus and $n$ is the electron density.

TABLE I. Peak-to-peak corrugations of the $10^{-3}$ Å$^{-3}$ electron-density contour, in Å. Column (a): superposition of free atomic densities (i.e., $\eta_{x,y} = 1$) with structure after Ref. 22. Column (b): $\eta_{x,y} = 0.79$, structure after Ref. 22. Column (c): $\eta_{x,y} = 0.85$, 26% relaxation.

| | (a) | (b) | (c) |
|---|---|---|---|
| [1$\bar{1}$0] | 0.09 | 0.03 | 0.05 |
| [001] | 1.55 | 1.15 | 1.22 |

which determines the extent of smoothing of the electron density along the close-packed rows, has been found to be negligible, and its value has therefore always been set equal to $\eta_y$.

For $\sigma = 2.6$ Å and $\eta_y = 0.79$, the behavior of the specular intensity as a function of $\gamma$ is quite accurately reproduced as shown in Fig. 3. It is to be noted that a few attempts to further improve the quality of the fit by choosing values of $A$ and $\beta$ different from the atomic values were unsuccessful. The calculated diffraction probabilities ($\triangle$) are shown in Fig. 1. Assuming an error of 10% in the experimental determination of the integrated diffraction intensities, we find a value of 13.6 for $\chi^2$, which indicates poor agreement. In general we expect the diffraction pattern to be more sensitive than the azimuthal pattern to higher Fourier components, i.e., the fine details, of the interaction potential. This appears to be the reason for the better agreement of the azimuthal pattern with theory.

As shown in Fig. 5 the He-(1×2)Au(110) interaction potential presents a well bottom localized between the rows of close-packed surface atoms at a distance of 2.4 Å from the topmost nuclear plane with local depth of 13.5 meV. This is about twice as large as the laterally averaged well depth which is only 6.83 meV. The equipotential surfaces show quite large corrugations along [001];

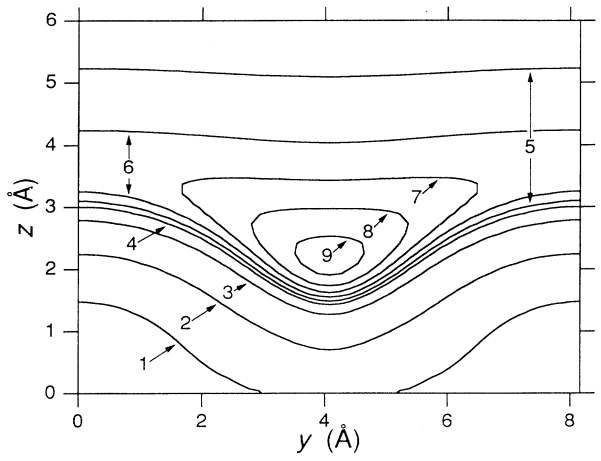


FIG. 5. Equipotential curves in the (1$\bar{1}$0) plane. The $z$ axis is perpendicular to the surface and the $y$ direction is along [001]. The origin is at the center of an atom in the top layer. 1, $10^3$ meV; 2, $10^2$ meV; 3, 10 meV; 4, 0 meV; 5, −2.5 meV; 6, −5 meV; 7, −7.5 meV; 8, −10 meV; 9, −12.5 meV.

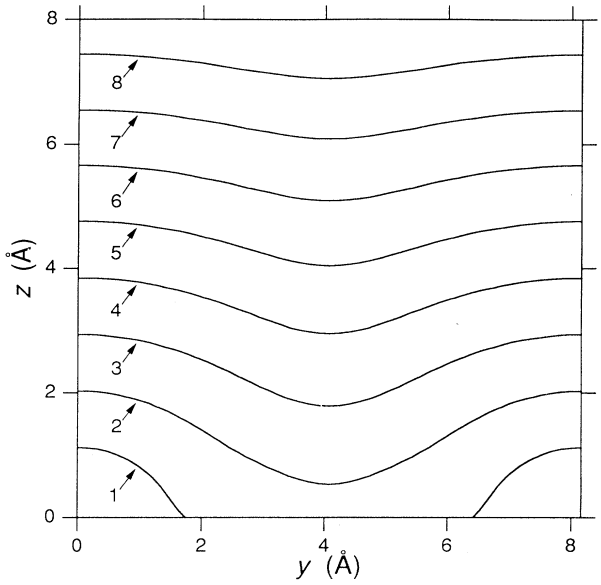


FIG. 6. Electron-density contours of the (1×2)-Au(110) surface in the (1$\bar{1}$0) plane. The $z$ axis is perpendicular to the surface and the $y$ direction is along [001]. The origin is at the center of an atom in the top layer. 1, $10^{-1}$ Å$^{-3}$; 2, $10^{-2}$ Å$^{-3}$; 3, $10^{-3}$ Å$^{-3}$; 4, $10^{-4}$ Å$^{-3}$; 5, $10^{-5}$ Å$^{-3}$; 6, $10^{-6}$ Å$^{-3}$; 7, $10^{-7}$ Å$^{-3}$; 8, $10^{-8}$ Å$^{-3}$.

in particular the peak-to-peak corrugation of the 20-meV equipotential surface is 1.2 Å. It is noticed that, due to the van der Waals interaction, the equipotential surfaces are substantially more corrugated than the isoelectron density surfaces reported in Fig. 6. In order to facilitate comparison with results which may be provided by scanning tunneling microscopy, the peak-to-peak corrugations along [001] and [1$\bar{1}$0] of the isoelectron density surfaces are given in Table I. Notice that the corrugation along [001] is strongly reduced from the value of 1.55 Å, column (a), to 1.15 Å, column (b).

### B. Structure

One of the advantages of He scattering is that it is nonpenetrating and therefore very surface sensitive. However, this very surface sensitivity makes it difficult to extract information about the surface structure, particularly for atoms below the top layer. In the present case, the top layer consists of the outermost atoms with a coordination number of 7; however, the atoms in the next layer down have a coordination number of 9, and those in the next layer, 11, and so they are also part of the surface. Generally it is assumed that helium scattering does not yield information about these atoms but since the present data are very detailed, we decided to investigate whether any such information could be extracted.

While most determinations of the structure of the (1×2)-Au(110) surface agree with the missing-row model, there is still some disagreement about the exact atomic displacements with respect to the ideally terminated sur-

face. Contractions in the spacing ($d_{12}$) between the first two layers of around 20% are usually found,[22,24–26] and theoretical predictions give a contraction from 16% to 27%.[27,28]

In the first step of our study, we assumed the geometrical structure of the Au(110) surface determined by Moritz and Wolf.[22] Figure 3, which was discussed above in connection with charge density, shows a comparison of the azimuthal scan with the theoretical curve. It is clear that there is overall agreement between the two curves with regard to peak position although the intensities vary a little. In the case of atom-surface scattering intensities, poor agreement between measured and calculated peak heights may be due to intensity losses in the experiment, associated with surface defects or inelastic events occurring during the relatively long time of interaction (of the order of $10^{-10}$ sec).[13] It is noted that these effects cannot be taken into account in a CCC calculation.

In order to obtain a realistic quantitative estimate of the optimization of the agreement between measured and calculated intensity curves, we used a simple modification of the position-dependent reliability-factor opposite sign (ROS) introduced by Van Hove, Tong, and Elconin[29] for low-energy electron diffraction (LEED). The modified opposite-sign reliability factor ($R_{\mathrm{MOS}}$) is given by

$$R_{\mathrm{MOS}} = A_{p1} \int \left(1 - \frac{I_e^{'}}{|I_e^{'}|} \frac{I_t^{'}}{|I_t^{'}|}\right) |I_e^{'}| d\gamma, \tag{4}$$

where $I_e^{'}$ and $I_e^{'}$ are the derivatives of the experimental and calculated intensities with respect to the azimuthal angle $\gamma$. The factor is made dimensionless by using the normalization[30]

$$A_{p1} = \frac{1}{2 \int |I_e^{'}| d\gamma}. \tag{5}$$

When performing the calculations with the Au surface atoms fixed in the positions given in Ref. 22 we find an $R_{\mathrm{MOS}}$ value of 0.2.

Next we varied the relaxation and other parameters in order to see how sensitive the calculated curve was to structural parameters. The overall results were that variations in the $\eta$ parameters of the topmost layer with respect to those of the other layers did not bring substantial improvements, lateral displacements in the second layer also were not significant, and variations in the distance between the second and third layer did not have a large effect. However, the most critical parameter for the missing-row structure is the relaxation $d_{12}$, and here we did see an effect.

The calculated $R_{\mathrm{MOS}}$ factor as a function of relaxation is shown in Fig. 7. The parameters $\sigma$ and $\eta_y$ have been adjusted for each value of $d_{12}$ in order to give the best fit. The minimum value of $R_{\mathrm{MOS}}$ occurs at a relaxation of 26%, where the parameters $\sigma$ and $\eta_y$ have to be set at 3.63 and 0.85, respectively. Moreover, much better agreement between the calculated diffraction probabilities and the experimental pattern is found in this case ($\diamond$ in Fig. 1, with a $\chi^2$ value of 5.03). No other structure gave a better value of $\chi^2$. This probably indicates that this structure yields a better determination of the higher

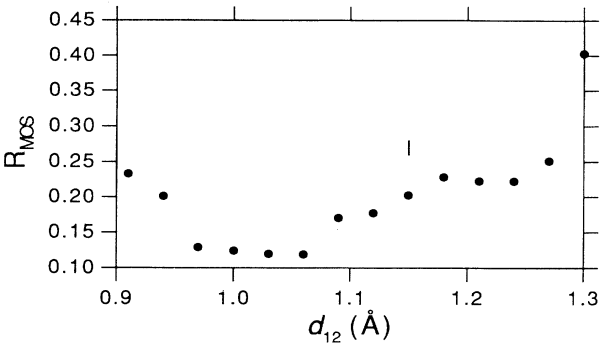


FIG. 7. $R$-factor $R_{\mathrm{MOS}}$ [Eq. (4)] plotted vs the first to second layer distance $d_{12}$. The vertical line marks the value obtained for the structure given in Ref. 22.

Fourier components of the interaction potential. In fact it is to be noted that the best fit is obtained with a significant decrease of the anisotropy of the atomic densities ($\eta_y = 0.85$ instead of 0.79), so that the peak-to-peak corrugation of the electron density remains very similar to the one obtained for the relaxation of Ref. 22—see Table I, columns (b) and (c).

The value of 26% for the $d_{12}$ contraction is larger than the value given in the literature, and we therefore conclude that the present method has an accuracy limited to ± 6%, or approximately 0.1 Å. This appears to be due to the limitations in the exact determination of the details of the potential. In particular only three parameters, $\sigma$ and $\eta_{x,y}$, may not be sufficient to fully describe the charge redistribution between the isolated atoms and the surface atoms. It seems that the surface atoms still appear too atomiclike and this would explain why the relaxation is ovestimated. Nevertheless, the present result shows that it is in fact possible to extract structural information from He-scattering data.

For the present it is very satisfactory that a fit using only three free parameters can achieve an accuracy of 6% in determining the interatomic positions. Further improvements in the accuracy of these data can be expected with improvements in the computational procedures and model potential.

## IV. CONCLUSIONS

Isoelectron densities and equipotentials for the He-Au(110) surface have been calculated and their accuracy tested by calculation of diffraction patterns and azimuthal patterns. The excellent agreement between theory and experiment shows the reliability of these calculations. The corrugation of the electron density and potential along the [1$\bar{1}$0] direction is negligible. In the orthogonal direction a corrugation of 1.3 Å is observed (20-meV equipotential), with a local well depth of 13.5 meV. The corrugation in the electron density is 1.2 Å. The calculations have also been applied to investigate the potential for structural determination using the azimuthal pattern. It is found that the missing-row structure fits the data and the distance between the first and second rows is found with an accuracy of 6%.

## ACKNOWLEDGMENTS

This work was supported by the Gruppo Nazionale di Struttura della Materia of the Consiglio Nazionale delle Ricerche (CNR) and by Centro Interuniversitario di Struttura della Materia of the Ministero della Istruzione (MPI). D.C. acknowledges a grant from AREA di Ricerca.

---

*Permanent address: Institute J. Stefan, Ljubljana, Slovenia.

[1]T. Engel and K.-H. Rieder, in *Structural Studies of Surfaces*, Springer Tracts in Modern Physics Vol. 91 (Springer, Berlin, 1982), p. 55.

[2]G. Comsa and B. Poelsema, *Scattering of Thermal Energy Atoms from Disordered Surfaces*, Springer Tracts in Modern Physics Vol. 115 (Springer, Berlin, 1989).

[3]E. Kirsten, G. Parschau, and K.-H. Rieder, Surf. Sci. Lett. **236**, L365 (1990).

[4]D. Cvetko, A. Lausi, A. Morgante, F. Tommasini, and K.C. Prince, Surf. Sci. **269/270**, 68 (1992).

[5]J. Lapujoulade, in *Interactions of Atoms and Molecules with Solid Surfaces*, edited by V. Bortolani, N.H. March, and M.P. Tosi (Plenum, New York, 1990), p. 381.

[6]P.J. Toennies, in *Dynamics of Gas-Surface Interactions*, edited by G. Benedek and U. Valbusa, Springer Series in Chemical Physics Vol. 21 (Springer, Berlin, 1982), p. 208.

[7]D. Cvetko, A. Lausi, A. Morgante, F. Tommasini, K.C. Prince, and M. Sastry, Measurement Sci. Technol. **3**, 997 (1992).

[8]M.G. Dondi, L. Mattera, S. Terreni, F. Tommasini, and U. Linke, Phys. Rev. B **34**, 5897 (1986).

[9]P. Cortona, M.G. Dondi, and F. Tommasini, Surf. Sci. Lett. **261**, L35 (1992).

[10]J. Lapujoulade, Y. Le Cruër, M. LeFort, Y. Lejay, and E. Maurel, Surf. Sci. **118**, 103 (1982).

[11]P. Cortona, M.G. Dondi, A. Lausi, and F. Tommasini (unpublished).

[12]J. Sprösser, B. Salanon, and J. Lapujoulade, Europhys. Lett. **16**, 283 (1991).

[13]E. Kirsten and K.-H. Rieder, Surf. Sci. **265**, 67 (1992).

[14]G. Mazzeo, G. Jug, A.C. Levi, and E. Tosatti, Surf. Sci. (to be published).

[15]J. Villain and I. Vilfan, Surf. Sci. **257**, 368 (1991).

[16]P. Cortona, M.G. Dondi, A. Lausi, and F. Tommasini, Surf. Sci. **276**, 333 (1992).

[17]P. Cortona, Phys. Rev. A **34**, 769 (1986).

[18]K.T. Tang and J.P. Toennies, J. Chem. Phys. **80**, 3726 (1984).

[19]E. Zaremba and W. Kohn, Phys. Rev. B **13**, 2770 (1976).

[20]N. Esbjerg and J.K. Nørskov, Phys. Rev. Lett. **45**, 807 (1980).

[21]M. Manninen, J.K. Nørskov, M.J. Puska, and C. Umrigar, Phys. Rev. B **29**, 2314 (1984).

[22]W. Moritz and D. Wolf, Surf. Sci. **163**, L655 (1985).

[23]G. Wolken, J. Chem. Phys. **58**, 3047 (1973).

[24]Y. Kuk, L.C. Feldman, and I.K. Robinson, Surf. Sci. **161**, L168 (1984).

[25]M. Copel and T. Gustafsson, Phys. Rev. Lett. **57**, 723 (1986).

[26]H. Hemme and W. Heiland, Nucl. Instrum. Methods B **9**, 41 (1985).

[27]K.-M. Ho and K.P. Bohnen, Europhys. Lett. **4**, 345 (1987).

[28]E. Tosatti (private communication).

[29]M.A. Van Hove, S.Y. Tong, and M.H. Elconin, Surf. Sci. **64**, 85 (1977).

[30]M.A. Van Hove, W.H. Weinberg, and C.-M. Chan, *Low-Energy Electron Diffraction*, Springer Series in Surface Science Vol. 6 (Springer, Berlin, 1986), p. 241.